On the Observation of 14 N Quadrupole Resonance Transitions in Water Proton NMR Relaxometry Dispersion Curves: The Case of a Labile NH Grouping in a Semirigid Molecular Moiety

Sabine Bouguet-Bonnet, Tristan Giraud, Loic Stefan, Marie-Christine Averlant-Petit, Daniel Canet

On the Observation of ^{14}N Quadrupole Resonance Transitions in Water Proton NMR Relaxometry Dispersion Curves. The Case of a Labile NH Grouping in a Semi-rigid Molecular Moiety

Sabine Bouguet-Bonnet[(1)], Tristan Giraud[(2)], Loic Stefan[(2)], Marie-Christine Averlant-Petit[(2)], Daniel Canet[(3)]*

(1) Université de Lorraine, CNRS, UMR 7036 CRM2, F-54000 Nancy, France

(2) Université de Lorraine, CNRS, UMR 7375 LCPM, F-54000 Nancy, France

(3) Université de Lorraine, CNRS, UMR 7563 LEMTA, F-54000 Nancy, France

KEYWORDS : ^{14}N NQR, NMR relaxometry, quadrupolar tensor, asymmetry parameter, NH correlation time, NH distance

ABSTRACT

The electric field gradient tensor (considered here at the level of a nitrogen nucleus) can be described by two parameters: the largest element in the (X,Y,Z) principal axis system, denoted by V_{ZZ} (leading to the nuclear quadrupole coupling), and the asymmetry parameter $\eta=(|V_{YY}| - |V_{XX}|)/|V_{ZZ}|$ with $|V_{ZZ}| > |V_{YY}| > |V_{XX}|$. The frequencies of the three nitrogen-14 NQR transitions depend on both parameters but, for sensitivity reasons, their determination may be especially difficult and time consuming. For a partly rigid NH grouping with a labile proton, water NMR relaxometry curves may exhibit these three transitions (dubbed quadrupolar dips or QRE) provided that the NH grouping belongs to a moiety possessing a sufficient degree of ordering. Their line-shape leads to the correlation time describing mainly the motion of the NH grouping (the proton of which being in exchange with water protons), and their amplitude can be interpreted in terms of an effective NH distance. This approach is applied to an hydrogel, where separate NQR lines are observed for the different types of water existing in this system. Furthermore, the analysis of experimental data allows one to determine the nuclear quadrupole coupling in the protonated and deprotonated forms of this molecular moiety involving a labile NH grouping.

INTRODUCTION

Nowadays, Nitrogen-14 Nuclear Quadrupole Resonance (NQR) is considered as an unambiguous means for the identification of nitrogen containing compounds noticeably explosives, drugs, pharmaceuticals… [1,2]. This capability arises from the fact that NQR relies on the interaction of the quadrupolar moment of a nucleus of spin greater than 1/2 (here, nitrogen-14 with a spin number equal to 1) with the electric field gradient (efg) due to the surrounding electrons. Thus, as the electron distribution within a molecular system is unique, the frequency of a NQR line is a true fingerprint of the considered compound. The technique, which is a magnetic resonance spectroscopy at zero field (it is the above-mentioned interaction which produces the energy level splitting), applies exclusively to solid state since, in the liquid state, the quadrupolar interaction averages to zero due to molecular tumbling. Moreover, the efg is a tensorial quantity which is defined only by two parameters because of the Laplace equation: the largest element in the efg (X,Y,Z) principal axis system, denoted by V_{ZZ}, and the asymmetry parameter $\eta = \frac{|V_{YY}|-|V_{XX}|}{|V_{ZZ}|}$ with $|V_{ZZ}| > |V_{YY}| > |V_{XX}|$. It is obvious that a proper characterization of the considered compound requires both V_{ZZ} and η. On the other hand, as will be detailed later, NQR of a spin 1 nucleus involves three transitions the frequency of which depends on V_{ZZ} and η. Evidently, the experimental determination of at least two of these frequencies appears indispensable. It turns out that the search of resonances (which may appear in a frequency range from a few hundreds of kHz to 6 MHz) for a new compound can be extraordinarily time consuming. For sensitivity reasons, the line at the highest frequency is obviously the less difficult to find out. Moreover, by analyzing the NQR spectrum obtained in the presence of a weak static magnetic field, it is relatively easy to determine V_{ZZ} and η from this single transition[3]. But the problem of finding this line remains difficult, especially when one is dealing with a nitrogen atom embedded in an environment which

is not fully rigid. This is precisely the problem addressed here in hydrogels formed by nucleobase-containing peptides (also termed nucleopeptides) [4]. In such hydrogels, it may happen that a given NH grouping of a nucleobase is partly immobilized and then able to produce NQR peaks at unpredictable frequencies due to the labile character of the NH grouping. Conversely, the measurement of these NQR frequencies should provide invaluable information about the dynamical properties at the level of this NH grouping. But, as already mentioned, these NQR lines are expected to occur at low frequency making their detection by pure NQR spectroscopy rather challenging. It turns out that, in such systems in aqueous solution, the proton of the NH grouping is generally labile thus exchangeable with the protons of water. Evidently, proton NMR (Nuclear Magnetic Resonance) of water is much more sensitive than NQR, and this is particularly true for relaxometry which consists of measuring the longitudinal relaxation rate R_1 as a function of the applied static magnetic field B_0 used in NMR experiments[5]. Relaxometry applied to water protons (generally through the so-called fast field cycling technique[6] at NMR frequencies ranging from some tens of kHz to some tens of MHz) leads to the characterization of slow motions experienced by water in complex systems. When there exists a dipolar interaction between water protons and a nitrogen nucleus located in a partly rigid environment (as described above), peaks are observed, superposed to the relaxometry curve (also called dispersion curve). These peaks are dubbed QRE (Quadrupole Relaxation Enhancement) or equivalently "quadrupolar dips" if T_1 ($1/R_1$) is plotted as a function of the proton resonance frequency. This phenomenon arises from dipolar relaxation between ^{14}N and ^{1}H and has been mostly observed and studied in proteins[7] where many NH groupings contribute to the QRE peaks. Here, we are dealing with large molecules in the liquid state, which nevertheless may possess NH groupings in a semi-rigid environment thus yielding QRE peaks. Although elaborate theories have been devised for treating quadrupolar dips[8] or QRE[9]

, and specifically in the case of immobilized proteins[10] (in a context quite different from the subject of the present study), we shall propose a simplified approach which confirms that these peaks occur really at the corresponding NQR frequencies. Furthermore, it will be shown that their line-shape can be interpreted according to the motions undergone by the considered NH grouping.

THEORY

Owing to the nature of the system investigated here, it seems reasonable to rest on the Bloch-Wangness- Redfield formalism for spin relaxation. Accordingly, we shall resort to this classical formalism for obtaining expressions of the ^{14}N-^{1}H dipolar contribution which adds to all other relaxation mechanisms acting on the water proton longitudinal relaxation rate.

A first simplistic (yet instructive) approach

It is well-known that the dipolar relaxation rate between a spin ½ A (water protons) and another spin ½ X can be expressed as

$$(R_1^A)_d = K_{AX}[6J(\omega_A + \omega_X) + 3J(\omega_A) + J(\omega_A - \omega_X)] \quad (1)$$

$$\text{with } K_{AX} = \left(\frac{1}{20}\right)\left(\frac{\mu_0}{4\pi}\frac{\gamma_A\gamma_X\hbar}{r_{AX}^3}\right)^2 \quad (2)$$

In the case of an isotropic reorientation (considered exclusively here) represented by a correlation time τ_c, the spectral density $J(\omega)$ has the simple form

$$J(\omega) = \frac{2\tau_c}{1+(\omega\tau_c)^2} \quad (3)$$

For the moment and temporarily (just for trying to understand the main features of our experimental observations), we shall assume the functional form of eq. (1) when X is a Nitrogen-14 nucleus. In our case, τ_c is assumed to be sufficiently large and K_{AX} small (with respect to other mechanisms affecting water longitudinal relaxation), so that the N-H dipolar relaxation is

negligibly small unless ω is zero. This obliviously occurs for the third term of (1) when, in a relaxometry experiment, the proton resonance frequency becomes equal to a nitrogen quadrupolar frequency (see figure 1 below). In such a situation, the spectral density is equal to $2\tau_c$ and therefore becomes significant (provided that the product $2\tau_c K_{AX}$ is sufficiently large with respect to all other contributions to proton longitudinal relaxation). In passing, we can realize that it is a similar process which explains that, in large molecules, R_2 (the transverse relaxation rate which involves a spectral density at zero frequency) is much larger than R_1 (which involves spectral densities at higher frequencies). This can be thought as the origin of "quadrupolar dips"/QRE, without the need to invoke a ^{1}H polarization transfer toward ^{14}N as stated in a relatively recent paper [11]. Moreover, it is obvious that the spectral density given by equation (3) is a simple Lorentzian line centered on ω = 0. In fact, concerning nitrogen and the frequencies currently investigated by proton relaxometry, such phenomena can only occur via NQR transitions which exist if and only if the quadrupolar interaction is not averaged to zero by fast molecular motions that is, in our case, if the NH vector is sufficiently rigid. At the B_0 values used in relaxometry experiments, Nitrogen-14 Zeeman splitting is so weak (the nitrogen resonance frequency ω_N is equal to $\frac{\gamma_N}{\gamma_H}\omega_H \sim 0.07\omega_H$, ω_H being the proton resonance frequency) that it can be neglected with respect to the quadrupolar splitting. Thus, the latter will be exclusively considered.

The NQR transitions are depicted in figure 1 where ω_Q is the NQR frequency expressed in $rad.s^{-1}$. $\omega_Q = 2\pi\nu_Q$ with the NQR frequency (expressed in Hz) $\nu_Q = \frac{eQ}{h}\frac{V_{ZZ}}{2}$, e being the electron charge, h the Planck constant and Q the ^{14}N electric quadrupole moment. The energy diagram, along with the three transitions for the case $\eta \neq 0$ ($0 \leq \eta \leq 1$), is also represented in figure 1. $\hat{I}_x$, $\hat{I}_y$ and $\hat{I}_z$ being the nitrogen-14 spin operators (here $\hat{I}^2 = 2$), $|+1\rangle, |0\rangle, |-1\rangle$ are the eigenvectors of the $\hat{I}_z$ operator.

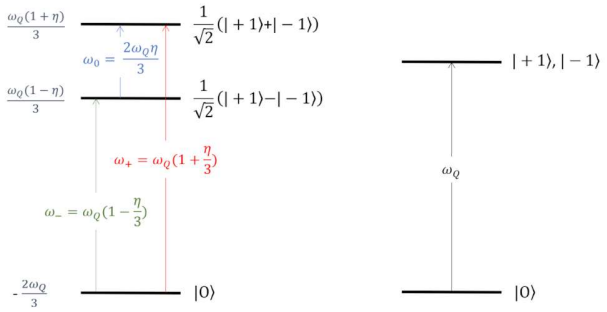

Figure 1. Left: the quadrupolar energy diagram along with the NQR transitions of a spin 1 in the general case. The energy values are indicated on the left of the energy levels and the eigenvectors on the right. Right: the energy diagram when the asymmetry parameter η is zero.

For the sake of simplicity, we first consider the case $\eta = 0$ for which a single NQR transition exists (figure 1, right). We are in a situation similar to that prevailing for equation (1) in the case of two nuclei of spin ½. However, because we are dealing with a spin 1, the coefficients in front of spectral densities have to be recalculated. Pragmatically, we shall replace the spectral density $J(\omega_A - \omega_X)$ by $J(\omega_H - \omega_Q)$ which is the only one we are interested in since it is responsible for the occurrence of the NQR line in the relaxometry curve. However, X (spin ½) is replaced by N (spin 1). Thus, the coefficient of $J(\omega_H - \omega_Q)$ is different from the coefficient of $J(\omega_A - \omega_X)$ in (1) and (2). Defining K_d as

$$K_d = \left(\frac{1}{20}\right)\left(\frac{\mu_0}{4\pi}\frac{\gamma_N\gamma_H\hbar}{r_{NH}^3}\right)^2 \qquad (4)$$

it is shown in the Supporting Information that the correct coefficient is $\left(\frac{\gamma_N}{\gamma_H}\right)\left(\frac{K_d}{6}\right)$.

A comprehensive approach for QRE/quadrupolar dips of a semi-rigid NH grouping

This approach, which rests on a practical strategy based on conventional spin relaxation calculations[12], is proposed in the Supporting Information and evidently applies to the general case ($\eta \neq 0$). It is shown that the contribution (to proton longitudinal relaxation) of the cross-relaxation parameter between water protons and the Nitrogen-14 nucleus has the general form given below (eq. (5)) and leads to the NQR lines through the spectral densities $J(\omega_H - \omega_+)$, $J(\omega_H - \omega_-)$ and $J(\omega_H - \omega_0)$. Of course, it can be used in its totality for complete simulations but this does not change the occurrence of the NQR lines.

$$R_1^{NH} = \left(\frac{\gamma_N}{\gamma_H}\right)\left(\frac{K_d}{6}\right)\{[J(\omega_H + \omega_+) + J(\omega_H - \omega_+)] + [J(\omega_H + \omega_-) + J(\omega_H - \omega_-)] + [J(\omega_H + \omega_0) + J(\omega_H - \omega_0)]\} \quad (5)$$

Note that this expression is in variance (although sharing the main features concerning the spectral densities but not their coefficients) with the one given in ref. 9. This is presumably due to the classical dipolar Hamiltonian used to obtain equation (5) (see the Supporting Information) whereas the expression of ref. 11 has for starting point a Hamiltonian based on random magnetic fields, acting on the proton of the NH grouping, created by ^{14}N magnetic moment. Indeed, it is not surprising that, in our eq. (5), the coefficients of spectral densities involving ω_+, ω_- and ω_0 are identical. This is due to the fact that ω_+ is associated with the x direction of the efg, ω_- with the y direction and ω_0 with the z direction (see the Supporting Information). As we are not dealing with a single crystal but with an isotropic medium, it appears that these three directions play the same role.

Finally, from the classical expression of spectral densities given by equation (3), it can be stressed that the linewidth at half-height of these NQR/relaxometry lines is equal to $1/(\pi\tau_c)$, thus the possibility to determine τ_c from the line-shape of these lines. The partner spectral density

$J(\omega_H + \omega_i)$ is also a Lorentzian function but centered at zero frequency. It therefore adds simply to the classical dispersion curve of water protons.

As a matter of fact, the three Lorentzian lines of each NH grouping leading to QRE will be treated according to the following expression, ν being the proton frequency in the dispersion curve and, with ν_Q the effective nitrogen quadrupolar coupling, $\nu_+ = \nu_Q(1 + \frac{\eta}{3})$, $\nu_- = \nu_Q(1 - \frac{\eta}{3})$, $\nu_0 = \nu_Q \frac{2\eta}{3}$

$$F(\nu) = A\left[\frac{1}{1+(2\pi\tau_c(\nu-\nu_+))^2} + \frac{1}{1+(2\pi\tau_c(\nu-\nu_-))^2} + \frac{1}{1+(2\pi\tau_c(\nu-\nu_0))^2}\right] \quad (6)$$

The amplitude A can be expressed according to (4) and (5). We obtain

$$A = \frac{\gamma_N^3\gamma_H}{60}\left(\frac{\mu_0\hbar}{4\pi}\right)^2 \frac{\tau_c}{r_{NH}^6} \quad (7)$$

Giving $A \sim 3.58\frac{\tau_c}{r_{NH}^6}$ where τ_c is expressed in μs while the effective NH distance, r_{NH}, is expressed in Å.

In practice, experimental data will be adjusted against A, ν_Q, η and τ_c. Thereafter r_{NH} will be deduced from A.

EXPERIMENTAL SECTION

^{1}H NMR relaxometry experiments were performed with a Stelar SMARtracer fast-field-cycling relaxometer (Stelar company, Medde, Italy) in a 5kHz-10MHz Larmor frequency range in 10-mm NMR tubes. For all R_1 measurements, magnetization recovery curves were found to be monoexponential within experimental errors. For each B_0 value, R_1 were obtained from the magnetization evolution as a function of time, sampled with 16 values between 0.01 and 4 times the longitudinal relaxation time. Different values of the static magnetic field were sampled, with a fixed acquisition field of 7.2 MHz (^{1}H Larmor frequency). Pre-polarized measurements were done

between 5kHz and 4MHz with a polarization duration of 1.5s and at a ^{1}H frequency of 8MHz, and non-polarized sequence was used between 4MHz and 10MHz. Field-switching time was 3ms.Temperature was fixed at 25°C, 35°C or 45°C.

For the complete dispersion profiles (from 5kHz to 10MHz), 32 different values of the static magnetic field were sampled, 8 accumulations were used and a recycle delay of 8s was applied.

Additional measurements were done in the 0.2-3.5MHz Larmor frequency range in order to obtain better resolution for the QRE peaks. For this goal, 128 different values of the static magnetic field were sampled between 1.35 and 3.50MHz and 64 between 0.25 and 1.35MHz. 8 accumulations were used with a recycle delay of 9s.

RESULTS AND DISCUSSION

As an example, we have investigated a hydrogel, or more precisely a supramolecular low-molecular weight peptide-based hydrogel[13,14], formulated from a nucleobase-containing peptide (also termed nucleopeptide). While four derivatives containing the four different DNA-nucleobases have been reported[15], they do not always exhibit the QRE phenomenon, and the guanine derivative displayed figure 2 has been selected herein. The NH grouping in the cycle located at the peptide nucleic acid form of the gelator is assumed to give rise to the QRE phenomenon displayed in figure 3.

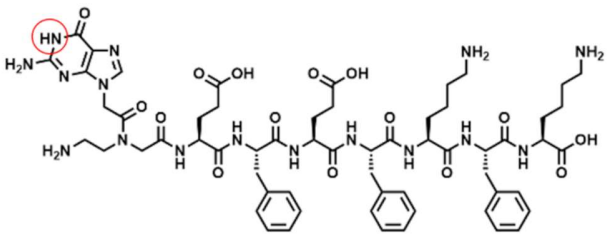

PNA(G)-EFEFKFK

Figure 2. The guanine-containing peptide molecule leading to the formation of the hydrogels which exhibit the QRE phenomenon. The NH grouping assuming to give rise to the QRE is highlighted in red.

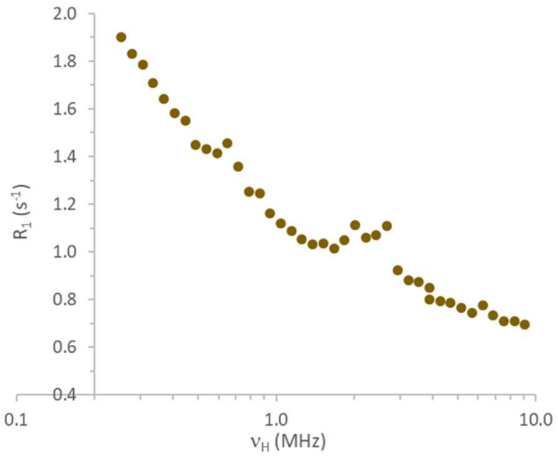

Figure 3. The experimental dispersion curve (semilogarithmic plot) exhibiting the QRE phenomenon for the hydrogel formed by the compound of figure 2 [15].

For investigating more accurately, the region of the dispersion curve involving the NQR (or QRE) peaks has been scanned (from 0.4 MHz to 3.5 MHz) with enhanced resolution and subtracted from the regular proton dispersion curve. Moreover, the frequency scale was made linear. The corresponding QRE spectrum is displayed in figure 4.

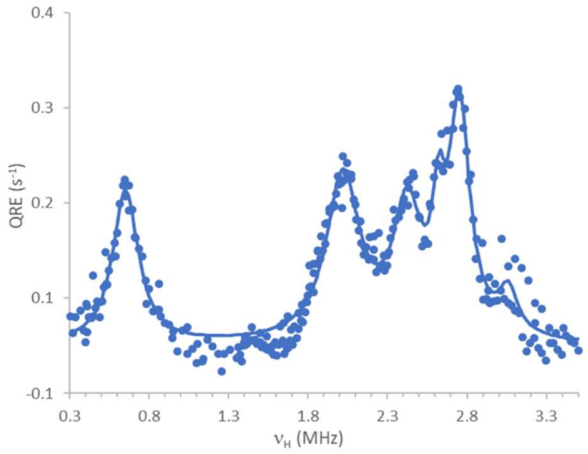

Figure 4. The "high resolution" QRE spectrum obtained by heavily zooming the corresponding region in figure 3. The regular proton dispersion curve has been subtracted. Dots: experimental data. Continuous curve: recalculated spectrum obtained with six lorentzians (see text).

Surprisingly and rather puzzling, in place of the three expected peaks (see eq. 6), we observe more numerous peaks: at 0.65 MHz, 2.01 MHz, 2.42 MHz, 2.75 MHz and 3.06 MHz, the peak at 2.75 MHz being seemingly composite. In fact, assuming that the peaks at 0.65 MHz and 2.01 MHz correspond respectively to ν_0 and ν_-, we find 2.66 MHz for ν_+ (because $\nu_+ - \nu_- = \nu_0$, see Fig.1) which would correspond (within experimental uncertainty) to the shoulder at 2.61 MHz. These three peaks will be assigned to NH_1 in the following. For interpreting the other peaks, we propose to define i) NH_2 with ν_+ around 2.75 MHz and ν_- at 2.42 MHz, ii) NH_3 with ν_+ around 3.06 MHz and ν_- at 2.75 MHz. It was also decided to treat the whole relaxometry curve from 0.1 MHz to 3.5 MHz without any pre-processing (as done before). This implies to adjust not only the QRE peaks but also the decay of the normal dispersion curve. It turned out that a proper fit was attained (figure 5a) with parameters concerning QRE peaks given in table 1. The peaks around 0.3 MHz

(NH_2 and NH_3, figure 5b) are almost invisible in the recalculated data (figure 5a), because they are blurred out by the genuine decay of the normal relaxometry dispersion curve.

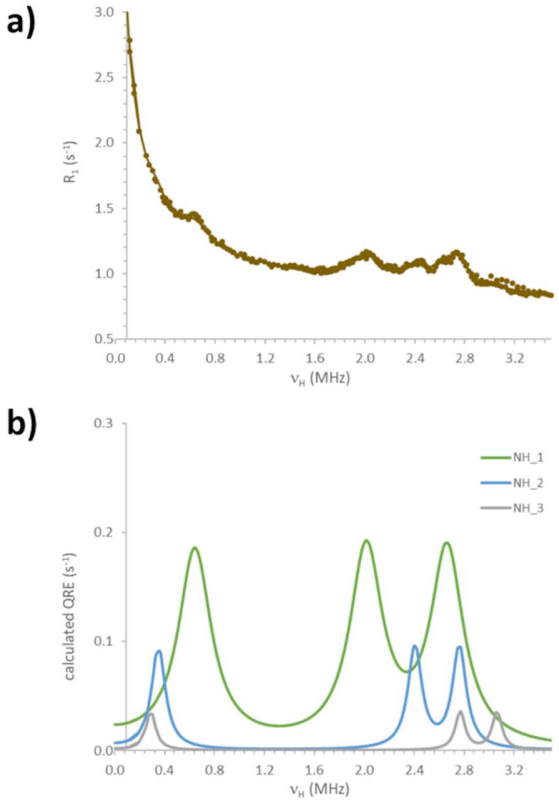

Figure 5. a) Dots: experimental NMRD data. Continuous curve: recalculated NMRD obtained with three different NH yielding QRE (see text). b) Separate recalculated QRE spectra for NH_1, NH_2, and NH_3.

	A (s^{-1})	ν_Q (MHz)	η	τ_c (μs)	r_{NH} (Å)
NH_1	0.18	2.34	0.41	1.00	1.65
NH_2	0.09	2.59	0.21	2.32	2.12
NH_3	0.04	2.92	0.15	3.31	2.64

Table 1. Parameters extracted from the analysis of the QRE spectrum

These results can be tentatively interpreted on the basis of the three types of water encountered in this hydrogel system as revealed by the analysis of the sheer dispersion curve[15]. These include bound water, a second hydration shell (less bound to the hydrogel) and free water. NH_1 would be assigned to bound water as it presents the expected behavior: three QRE peaks with a nuclear quadrupolar coupling indicating possibly the involvement of a deprotonated form which is expected due the lability of the NH grouping (see below). Bound water is expected to exchange rapidly with the proton of the NH grouping and the effective r_{NH} (affected by the exchange rate) is just slightly larger than the NH distance in a non-labile NH grouping (around 1Å). Moreover, the correlation time τ_c should be also related to the exchange rate. These latter considerations apply as well to NH_2 and NH_3. It appears that r_{NH} is longer for the second hydration shell and still longer for free water. Likewise, higher correlation times are found indicating consistently smaller exchange rates. Thus, the time needed by water protons to reach the nitrogen atom is larger for NH_2 and NH_3. During this longer period, the molecule can be re-protonated and, thus, water interacts partly with the unmodified molecule. Conversely, in the case of NH_1, water seems to interact essentially with the deprotonated molecule. In fact, NH_1, NH_2 and NH_3 are subjected to an average between protonated and deprotonated molecules with a more pronounced contribution of the protonated molecule when going from NH_1 to NH_3.

Finally, we have investigated the evolution of the QRE peaks as a function of temperature mainly to probe a possible evolution of the hydrogel structure. This can be visualized in figure 6. The major feature is a remarkable invariant of the spectrum except its intensity which decreases when temperature increases.

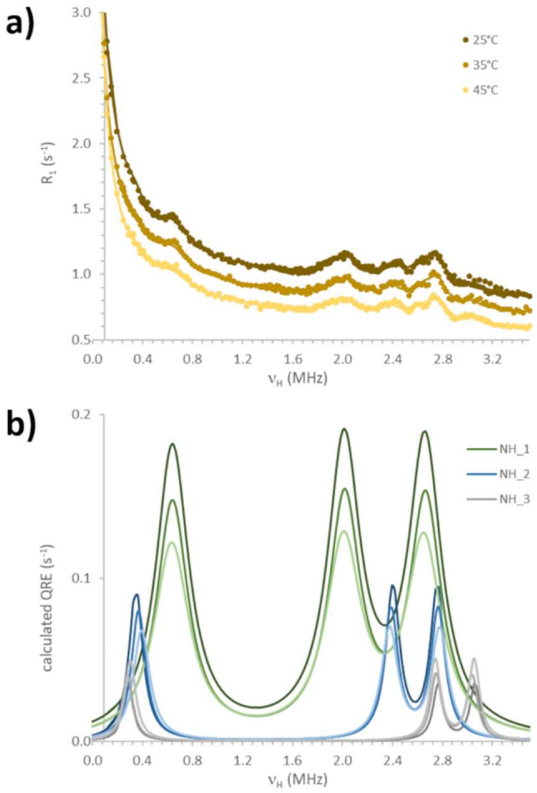

Figure 6. a) experimental (dots) and recalculated (continuous lines) NMRD data at 25°C, 35°C and 45°C. b) recalculated QRE spectra for NH_1 (green), NH_2 (blue), and NH_3 (grey), as a function of temperature (at 25°C, 35°C and 45°C, from dark to light color).

		A (s^{-1})	ν_Q (MHz)	η	τ_c (μs)	r_{NH} (Å)
25°C	**NH_1**	0.18	2.34	0.41	1.00	1.65
	NH_2	0.09	2.59	0.21	2.32	2.12
	NH_3	0.04	2.92	0.15	3.31	2.64
35°C	**NH_1**	0.15	2.35	0.41	1.04	1.71
	NH_2	0.08	2.58	0.22	2.28	2.16
	NH_3	0.04	2.90	0.15	3.10	2.54
45°C	**NH_1**	0.12	2.34	0.41	0.93	1.74
	NH_2	0.07	2.59	0.23	1.97	2.17
	NH_3	0.05	2.91	0.16	3.01	2.45

Table 2. Parameters extracted from the analysis of the QRE spectra

Parameters concerning QRE as a function of temperature are given in table 2. ν_Q and η are seen to be almost independent of temperature, indicating that the hydrogel structure does not change in this temperature range (below the sol-to-gel transition temperature of 49.5°C[15]) . At first sight, the independence of τ_c with respect to temperature is rather intricate as it is a dynamical parameter. As we have already seen, it is related to the exchange rate of the labile proton but it is primarily related to the motion of the vector joining H_2O to the nitrogen atom. The large value of this correlation time indicates a very slow motion which can only be ascribed to the hydrogel fibers (previously observed by TEM[15]). Therefore, the invariance of τ_c with temperature confirms that the structure of these fibers does not change in the investigated temperature range. On the other hand, the increase of r_{NH} with temperature (consequence of the decrease of the amplitude of the QRE peaks and the invariance of τ_c) can be thought as reflecting the increase of thermal motion affecting H_2O (also confirmed by the evolution of the full dispersion curves with temperature).

Calculation of quadrupole couplings and asymmetry parameters

In order to get further insight in the interpretation of our experimental results, we have undertaken theoretical calculations by modifying and simplifying the well-known Townes-Dailey approach[16]. Basically, Townes and Dailey demonstrated that only valence p-atomic orbitals have to be considered for the calculation of the efg tensor. More precisely, these calculations were carried out from the coefficients of these atomic orbitals in molecular orbitals. Quite recently[17], the Townes-Dailey model has been extended for a better visualization of efg tensors. We propose here a simpler approach which makes exclusively use of (2s)-(2p) hybrid atomic orbitals adapted to the geometry of the molecular moiety which contains the NH grouping under investigation (and not molecular orbitals) including the Slater formulation for the radial part and spherical harmonics

for the orientational part. We shall rely on the NQR frequency ν_Q and on the asymmetry parameter η . Their estimation implies the calculation of the electric field gradient along the efg principal axes which are assumed to be known by symmetry or pseudo-symmetry reasons. Each calculation results in the product of a radial integral by an angular integral (these integrals can be easily carried out by hand). A major advantage of Slater orbitals originates from the *same* radial part for (2s) and (2p) atomic orbitals thus for any hybrid orbital. Therefore, the *same* radial integral will constitute a *common factor* in all terms of the calculated electric field gradient. However, Slater orbitals depend critically on an effective atomic number (Z^*) which accounts for the shielding effect due to all electrons less the electron described by the considered Slater orbital. In spite of the approximations inherent to Slater orbitals, their reliability has been recognized for a long time. In the present context, various tests concerning calculations of the efg tensor as a function of the nitrogen hybridization led to very satisfactory results (our method will be detailed in a separate report). Finally, it can be noted that, in the calculation of the asymetry parameter, the radial integral simply disappears making the determination of η by this method especially safe.

For now, we just mention the results of this strategy for the situations encountered in the present work. For the protonated form, one has: ν_Q = 3.21MHz and η = 0 while for the deprotonated form ν_Q = 2.40 MHz and η = 0.40. Thus, it appears that, for NH_1, one should have exclusively the deprotonated form while the protonated form should be present in NH_2 and NH_3.

Now, with the help of these theoretical results, we can go further by relying on the experimental data given in table 1. We shall only keep the values of asymmetry parameters: $\eta = 0.41$ for the deprotonated species and η close to zero for the protonated species, essentially, as mentioned above, because these quantities depend only on the spherical harmonics involved in hybrid atomic orbitals and can therefore considered as especially reliable. As stated before, the results of table 1

are an average of protonated and deprotonated forms and can be expressed according to the proportion $p = \frac{\eta}{0.41}$ of the deprotonated form. One can always write

$$\nu_Q = p\nu_d + (1-p)\nu_p \qquad (8)$$

where ν_d and ν_p stand for the nuclear quadrupole coupling in the deprotonated form and in the protonated form, respectively. These two quantities have been determined by least-squares from NH_1, NH_2 and NH_3 yielding $\nu_d = 2.31\ MHz$ and $\nu_p = 3.13 MHz$. Experimental and recalculated values of ν_Q along with the value of p are given in table 3. Moreover, it can be seen that ν_d and ν_p are in agreement (just slightly smaller) with the theoretical values given above. This is a remarkable result indicating that the approximations of our theoretical approach are especially valid.

	ν_Q exp (MHz)	ν_Q calc (MHz)	p
NH_1	2.34	2.32	1.00
NH_2	2.59	2.71	0.50
NH_3	2.92	2.82	0.37

Table 3. Experimental and recalculated nuclear quadrupole couplings with specific nuclear quadrupole coupling for deprotonated and protonated forms at 25°C: $\nu_d = 2.32\ MHz$ and $\nu_p = 3.11 MHz$. p is the proportion of the deprotonated species.

Moreover, the value found for the protonated molecule turns out to be close to that of guanine calculated by full quantum chemistry calculations[18]. As the NH grouping under investigation belongs to a molecular fragment resembling guanine (see figure 2), it can be thought that the semi-rigidity of that molecular moiety does not affect the NQR frequency and that all goes as if it were

totally rigid. However, this feature prevents us to determine the degree of rigidity of the considered molecular moiety.

CONCLUSION

This study has emphasized that the QRE phenomenon, when it exists, is invaluable for directly and easily obtaining the NQR frequencies (providing the apparent quadrupole coupling constant) and thus attesting some degree of rigidity of the NH grouping in systems (as the hydrogel investigated here) a moiety of which is neither in the liquid state, nor in the solid state. It has been pointed out that these quadrupolar lines are Lorentzian, with a linewidth at half-height equal to $1/(\pi\tau_c)$, τ_c being a correlation time characterizing the mobility of the NH grouping. On the other hand, the amplitude of these Lorentzian lines leads to an effective NH distance that increases when the exchange rate affecting the labile amide proton decreases, as observed with the different types of water present in this system. Moreover, investigations of the QRE lines as a function of temperature indicate that the structure of hydrogel fibers does not change in the investigated temperature range (25°C-45°C, below the sol-gel transition). Only the thermal motion affecting the water molecules (solvent) increases with temperature. It has also been possible to determine the nuclear quadrupole couplings in the protonated and deprotonated forms in agreement with a new theoretical approach developed to understand the differences between protonated and deprotonated forms. It must be noticed that these relaxometry experiments, when they exhibit QRE peaks, provide more information than pure NQR spectra, the observation of which risking in any case to be jeopardized by exchange phenomena.

ASSOCIATED CONTENT

Supporting Information. The following file is available free of charge: details of the theoretical calculations for the QRE lines observed in relaxometry experiments (PDF file).

AUTHOR INFORMATION

Corresponding Author

* Sabine.Bonnet@univ-lorraine.fr

Author Contributions

The manuscript was written through contributions of all authors. All authors have given approval to the final version of the manuscript.

TOC GRAPHIC

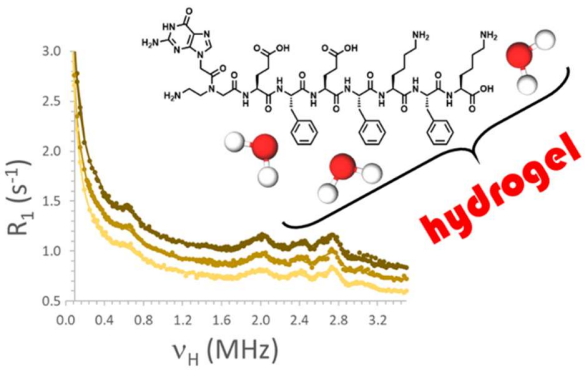

ACKNOWLEDGEMENTS

L.S and M.-C.A.-P acknowledge the Centre National de la Recherche Scientifique (CNRS) for funding. L.S. thanks the Agence National de la Recherche (ANR-20-CE06-0010-01 MUNCH)

for funding. T.G. thanks the Ministère de l'Enseignement Supérieur, de la Recherche et de l'Innovation (MESRI) for his Ph.D. grant.

REFERENCES

(1) Fraissard, J.; Lapina, O. Explosives Detection Using Magnetic and Nuclear Resonance Techniques, Springer, Berlin, 2009.

(2) Barras, J.; Murnane, D.; Althoefer, K.; Assi, S.; Rowe, M. D.; Poplett, I. J. F.; Kyriakidou, G.; Smith, J. A. S. Nitrogen-14 nuclear quadrupole resonance spectroscopy: A promising analytical methodology for medicines authentication and counterfeit antimalarial analysis. *Anal. Chem.* **2013**, *85*(5), 2746-2753.

(3) Aissani, S.; Guendouz, L.; Canet, D. N-14 Quadrupole Resonance in the presence of a weak static magnetic field. Direct determination of the electric field gradient tensor. *Chem. Phys. Lett.* **2014**, *594*, 13-17.

(4) Giraud, T.; Hoschtettler, P.; Pickaert, G.; Averlant-Petit, M.C.; Stefan L. Emerging low-molecular weight nucleopeptide-based hydrogels: state of the art, applications, challenges and perspectives. *Nanoscale* **2022**, *14*, 4908-4921.

(5) Kimmich, R. NMR Tomography, Diffusometry, Relaxometry, Springer, Berlin, 1997.

(6) Kimmich, R. Field-cycling NMR Relaxometry, Royal Chemical Society, Cambridge, 2019.

(7) Kruk, D.; Florek-Wojciechowska, M. Recent Development in ^{1}H NMR Relaxometry *Annu. Rep. NMR spectrosc.* **2020**, *99*, 119-184. And references therein.

(8) Winter, F.; Kimmich, R. Spin lattice relaxation of dipole nuclei (I = 1/2) coupled to quadrupole nuclei (S = 1). *Mol. Phys.* **1982**, *45*(1), 33-49.

(9) Fries, P.H.; Belorizky, E. Simple expressions of the nuclear relaxation rate enhancement due to quadrupole nuclei in slowly tumbling molecules. *J. Chem. Phys.* **2015**, *143*, 044202.

(10) Sunde E.P.; Halle B. Mechanisms of ^{1}H-^{14}N cross-reaxation in immobilized proteins, *J. Magn.* Reason. **2010**, *203*, 257-273.

(11) Kruk, D.; Masiewicz, E.; Borkowska, A. M.; Rochowski, P.; Fries, P. H.; Broche, L.M.; Lurie, D.J. Dynamics of Solid Proteins by Means of Nuclear Magnetic Resonance Relaxometry. *Biomolecules* **2019**, *9(11)* 652.

(12) Canet, D. Cross-relaxation and Cross-correlation Parameters in NMR: molecular approaches, Royal Chemical Society, Cambridge, 2018, pp. 32-34.

(13) Mondal, S.; Das, S.; Nandi A.K. A review on recent advances in polymer and peptide hydrogels. *Soft Matter* **2020**, *16*, 1404-1454.

(14) Das, R.; Gayakvad, B.; Shinde, S.D.; Rani, J.; Jain, A.; Sahu, B. Ultrashort Peptides - A Glimpse into the Structural Modifications and Their Applications as Biomaterials. *ACS Appl. Bio Mater.* **2020**, *3(9)*, 5474–5499.

(15) Giraud, T.; Bouguet-Bonnet, S.; Marchal, P.; Pickaert, G.; Averlant-Petit, M.-C.; Stefan, L. Improving and fine-tuning the properties of peptide-based hydrogels via incorporation of peptide nucleic acids. *Nanoscale* **2020**, *12*, 19905-19917.

(16) Townes, C. H.; Dailey, B.P. Determination of Electronic Structure of Molecules from Nuclear Quadrupole Effects. *J. Chem. Phys.* **1949**, *17*, 782-796.

(17) Rinald, A.; Wu, G. A Modified Townes-Dailey Model for Interpretation and Visualization of Nuclear Quadrupole Coupling Tensors in Molecules. *J. Phys. Chem. A* **2020**, *124(6)*, 1176-1186.

(18) Russo, N.; Sicilia, E.; Toscano, M.; Grand, A. Theoretical prediction of nuclear quadrupole coupling constants of DNA and RNA nucleic acid bases. *J. Molec. Struct.* **2001**, *563-564*, 125-134